NUCLEAR MASSES AND NUCLEAR STRUCTURE

N. Zeldes

The Racah Institute of Physics, The Hebrew University of Jerusalem

Abstract

We discuss microscopical interpretations of nuclear mass systematics, emphasizing aspects having relevance to nuclei far from stability.

Contents

1. Introduction
   - 1.1 Structural effects in masses. Plan of the talk
   - 1.2 Properties of the effective nucleon-nucleon interaction
2. Few-nucleon clusters
   - 2.1 Splitting of the mass surface and nucleon pairing
   - 2.2 The Wigner term and neutron-proton isopairing
   - 2.3 Remarks on quartet correlations
3. Shells and subshells
   - 3.1 On the relation of shell effects in nuclear masses and excitation energies to gaps in single-nucleon spectra.
   - 3.2 Variation of the strength of magic numbers: mutual support of magicities
   - 3.3 Variation of shell effects at submagic numbers
4. Deformation
   - 4.1 Deformation regions
   - 4.2 Change of the magic number scheme with deformation
   - 4.3 Oscillating trends in the masses and deformation

1. Introduction

1.1 Structural effects in masses. Plan of the talk

The theme of my talk is the relation of the structure of the nuclear mass surface to nuclear structure, emphasizing mainly aspects related to nuclei far from stability. In this connection, structure of the mass surface refers to deviations from smooth overall behaviour as shown in fig. 1. Conspicuous among these are:

a. Splitting of the nuclear mass surface into four sheets according to parity type (even-even, odd-even, etc.)

b. Discontinuous change of slope along the line Z = N (Wigner term in mass equations)

c. Discontinuities of slope along magic number lines in the (N,Z) plane, and also sometimes along submagic lines.

d. Oscillations of the mass surface between magic number lines.

Likewise, by nuclear structure we mean microscopic structure, determined by clustering and correlated motion of nucleons. We are not concerned with gross structure considered in the liquid-drop model. Corresponding to the above four features of the mass surface, and related to them in the corresponding order, one finds the following microscopic substructures, of increasing complexity:

a. Identical nucleon pairs with $J_{12} = 0$.

b. Neutron-proton pairs with $T_{12} = 0$.

c. Formation of spherical shells and subshells.

d. Deformation of the shells.

The first two are two-nucleon clusters, whereas the last two are many-nucleon structures. They are considered in the following in the above order.

Preceding this, we briefly summarize in sect. 1.2 the properties of the effective nucleon-nucleon interaction as described by Schiffer[1]. This description is very useful for understanding and interrelating the phenomena discussed here.

1.2 Properties of the effective nucleon-nucleon interaction

Schiffer[1] derived effective nucleon-nucleon interaction matrix elements from experimental two-nucleon spectra and masses, and plotted them together as function of the quasiclassical angle θ between the angular momenta of the two nucleons. His results for nucleons in the same shell are shown in fig. 2. The data nicely divide into two groups, comprising the T = 1 (even J) and T = 0 (odd J) cases. For T = 1 there is only one strongly bound state at $\theta = \pi$, corresponding to antiparallel J = 0 pairing of the nucleon spins. On the other hand, for T = 0 the aligned J = 2j state with $\theta \simeq 0$, and also the quasipaired J = 1 state, are strongly bound, and the average interaction in the T = 0 states is altogether lower (more attractive) than for T = 1.

The situation in the case of two nucleons in different shells is similar.

2. Few-Nucleon Clusters

2.1 Splitting of the mass surface and nucleon pairing

Two identical nucleons can only be in T = 1 states. It was mentioned above that of these only the paired J = 0 state is strongly bound. Consequently, the ground state of semi-magic nuclei always contains the highest allowed number of paired $|j^2 J=0\rangle$ valence nucleons. This is the (maximum-) pairing or lowest-seniority approximation. On the other hand, also in mixed valence shells one expects large lowest-seniority components in the ground state wave function of nuclei not too-far removed from doubly-closed shells.

This leads in a natural way to splitting of the mass surface into four sheets, with the odd-N, odd-Z and odd-odd surfaces lying at respective distances of $-\frac{1}{2}\pi_n$, $-\frac{1}{2}\pi_p$ and $-\frac{1}{2}\pi_n - \frac{1}{2}\pi_p + I'$ above the even-even surface, where π_n and π_p are respectively the (negative) neutron and proton pairing energies, and I' is the (negative) higher-multipole interaction between the odd neutron and odd proton. Due to this interaction the odd-odd surface lies at a smaller distance from the odd-A surfaces than the even-even surface. The splitting of the mass surface is shown in fig. 3, where one observes that the vertical distance between the Rh parabolas is smaller

than for Pd, due to the I' term. A similar situation is observed in fig. 5 below.

2.2 The Wigner term and neutron-proton isopairing

When there are both neutrons and protons in the valence shells one expects to find many neutron-proton pairs in isopaired T = 0 states. This favours a low total isospin. As a matter of fact, nuclear ground states have as a rule* the lowest possible isospin, namely $T = |T_Z| = \frac{1}{2}|N-Z|$.

The sum over all valence nucleon pairs of the isoscalar $(\underline{t}_1 \cdot \underline{t}_2)$ component of the effective interaction leads to a symmetry energy proportional to $T(T+1)$. Since $T_{g.s.} = \frac{1}{2}|N-Z|$ this has cusp discontinuity along the line Z = N, as shown in fig. 4.

2.3. Remarks on quartet correlations

Several experimental facts about nuclear masses suggest possible existence of two-neutron-two-proton substructures in nuclei, which are called quartets[3]. On the other hand, the above regularities can also be interpreted by the lowest-seniority approximation based on pairing alone[3-5].

Spatial symmetrically correlated quartets are assumed in the supermultiplet approximation[6]. There has been considerable discussion recently[6] of the applicability of this assumption to nuclear ground states, with mainly non-conclusive results.

In a simple version of the supermultiplet approximation, assuming long range Wigner and Majorana effective interactions, one obtains symmetry energy proportional to T(T+4), and splitting according to parity such that the odd-A surface is situated midway between the even-even and odd-odd surfaces. Additionally, the pairing and symmetry coefficients are proportional to each other. It was found recently[7] that this supermultiplet description of symmetry and pairing energies is superior to that of the liquid drop picture. On the other hand, it has been claimed[5,8] that the T(T+1) symmetry term of the pairing-isopairing approximation and the latter's description of the splitting by independent coefficients, resulting in an odd-odd surface which is nearer to the odd-A surfaces than the even-even surface, are in better agreement with the data.

The determination of the ratio of the linear and quadratic terms in T from the data is more significant when using data reaching to the Z = N line. Thus mass determination of heavier Z = N nuclei far from stability is highly relevant to comparative study of the usefulness and range of validity of the above discussed models.

3. Shells and subshells

3.1. On the relation of shell effects in nuclear masses and excitation energies to gaps in single-nucleon spectra

Fig. 5 shows discontinuities in the slope of the mass surface at the magic numbers N = 20 and N = 126. In the lower part of the figure one observes sudden drops in the two-neutron separation energies at these numbers, which are an equivalent manifestation of the slope changes in the masses.

One is conveniently inclined to associate such sudden drops in separation energies with the beginning of new shells. This interpretation is based on the zeroth-order approximation (in the sense of perturbation theory) of the shell model, where one assumes that the nucleons are moving independently of each other in an average potential field created by their effective interactions. In this approximation the energy is the sum of single-nucleon shell energies, $E^{(0)} = \Sigma\varepsilon_{nlj}$. Neglecting rearrangement effects, the separation energy of the last neutron (proton) is equal to minus its energy ε_{nlj} of the last filling shell, and is constant in a chain of isotopes (isotones) having the same valence neutron (proton) shell. On the other hand, when a new shell starts to fill, the separation energy decreases by the energy difference of the two shells. This is illustrated in fig. 6.

On the other hand, empirical separation energies in chains of isotopes or isotones display strong odd-even oscillations of about 2 MeV, superimposed on monotonous variation with N and Z, of somewhat smaller magnitude. This is seen in the lower part of fig. 3 for Sn as function of N in the Rh and Pd isotopes, and in fig. 7 for Sp as function of N in Zr, Nb, Mo and Tc isotopes. These MeV differences between experimental and zeroth-order separation energies are due to the thus far neglected residual interactions between the nucleons, like those plotted in fig. 2, which are considered in the higher-order approximations of the shell model.

Likewise, there are differences of the above order of magnitude in excitation energies. In the zeroth-order approximation the energy depends only on the occupied shells and is highly degenerate, whereas empirically the splitting apart of the levels of a nuclear configuration usually exceeds the (zeroth-order) energy difference between neighbouring configurations. This is illustrated in fig. 8, showing the levels of the nuclear $lp_{3/2}^2$ configuration. Rather than being degenerate, their span in energy is about 5 MeV in ^{6}Li.

Thus, while one might reasonably relate in a qualitative way discontinuities in separation and excitation energies to gaps in the single-nucleon spectrum, as we often do in the following, quantitative conclusions can not be reliably drawn from such comparisons without further detailed calculations taking into account the residual effective interaction appropriate for the potential assumed at the start of the shell model perturbation treatment.

As a matter of fact, both the nuclear potential with its single-nucleon levels and gaps, and the residual two-body interaction, do not have precise physical meaning. They are mathematical constructs, obtained by somewhat arbitrarily separating the nuclear Hamiltonian into two parts. Consequently, single-nucleon energy gaps acquire a precise meaning only in relation to the assumed nuclear potential.

3.2. Variation of the strength of magic numbers: mutual support of magicities.

Large slope discontinuities at given nucleon numbers accompanied by large drops of separation energies as seen in fig. 5 are observed at nucleon numbers N,Z = 2,8,20,28,50,82 and N = 126. These are the official magic numbers. Smaller discontinuities in smaller groups of nuclei occur at the submagic numbers N,Z = 14, N = 56, 152 and Z=40,64. There is also some submagic behaviour at N = 98, 104, 108.

We consider in this section variations of neutron magic discontinuities with proton number and vice versa. Submagic discontinuities are similarly

*) Violation of this rule in heavier odd-odd Z=N nuclei is discussed in ref[2].

considered in the next section. A systematic study of these effects was recently made by Dr. Schmidt[9] at G.S.I.

We base the discussion on the behaviour of odd-nucleon separation and excitation energies with respect to an even-even core, as the interpretation of these in terms of odd-nucleon transitions is most straight forward. We start with the highest magic numbers, N = 126 and Z = 82.

The lower part of fig. 9 shows Sn systematics of odd-N nuclei near doubly-magic ^{208}Pb. The gap above N=126 is manifested as abrupt drop of isotopic S_n lines between N = 125 and N = 127. This drop increases from Hg to Pb*, and decreases again from Pb to Po and to Rn.

The upper part of the figure shows the excitation energy of the 125th neutron from the g.s. single-neutron $\frac{1}{2}^-$ level to the single-neutron $9/2^+$ level in the next major shell. This likewise increases from Hg to Pb and decreases again in Po. Furthermore, the shown excitation energy of the single neutron-hole $\frac{1}{2}^-$ level in N = 127 nuclei from their g.s. single-neutron $9/2^+$ level, involving the same neutron transition across the gap into the next major shell, likewise decreases from Pb to Po.

Thus, both the drop in separation energy and the inter-shell excitation energy across the neutron gap attain their maximum value at magic proton number Z = 82.

Analogously, the lower part of fig. 10 shows Sp systematics of odd-Z nuclei near ^{208}Pb. The proton magic gap above Z = 82 is manifested as sudden drop of isotonic S_p lines between Tl and Bi. The drop increases from N = 120 to N = 126 and decreases again in N = 128 and N = 130**.

Likewise, the upper part of fig. 10 shows excitation energies of the 81th proton in Tl isotopes, from the g.s. single-proton $\frac{1}{2}^+$ level to the single-proton $9/2^-$ level in the next major shell, and excitation energies of single proton-hole $\frac{1}{2}^+$ states from the g.s. $9/2^-$ level in Bi isotopes. The proton transition occurs in both cases across the gap into the higher major shell, and the data indicate that the energy change involved reaches its maximum value at magic neutron number N = 126.

The common conclusion from both figs. 9 and 10 is that near doubly-magic ^{208}Pb magic effects of a given kind of nucleons attain their maximum strength for a magic number of nucleons of the other kind. Schmidt et al[9] call this effect mutual support of magicities, and find that it occurs quite generally near doubly magic and submagic nuclei.

We now discuss possible interpretations of the effect, starting with the zeroth-order independent-particle picture described in sect. 3.1.

The upper part of fig. 11 shows schematically valence neutron and proton single-nucleon levels near ^{208}Pb, having low spin values just below their respective gaps, and high spin-values just above them.

* This statement is based on S_{2n} systematics. The experimental Sn value of ^{207}Hg, which is missing in the figure, is presently unknown.

** This statement is based on S_{2p} systematics. The experimental S_p values of ^{209}Tl and ^{211}Tl which are missing in the figure, are presently unknown.

When protons are added from Hg to Pb and then to Po, the nuclear radius increases and the symmetry energy decreases. These changes increase the binding energy of neutrons and lower their single-particle levels.

In order to account for the observed variation of neutron magicity with Z in this way, the variation of the neutron potential from Hg to Pb has to be such, that the last neutron level below the gap is lowered more than the first neutron level above the gap, thus increasing the neutron gap in Pb as compared to Hg. On the other hand, further variation of the neutron potential from Pb to Po should reverse the relative downward shift of the above neutron levels, decreasing the gap again in Po. Such level movements are shown in the lower part of fig. 11.

Such variations of level spacings do not occur in conventional simply parametrized potentials, with smooth A and I dependence.

On the other hand, spherical Hartree-Fock-Bogoliubov calculations like those reported by Prof. Sorensen at this conference[10], although producing shifts of levels, likewise fail to reproduce the variations of magicities observed in figs. 9 and 10.

Thus, quantitative explanation of the mutual support of magicities presently seems to present a challenge to Hartree-Fock theories.

On the other hand, the effect is presumably naturally reproducible by considering explicitly the neutron-proton residual interaction in first order shell model calculation. Then, due to radial and angular overlaps of the single nucleon wave functions, the average neutron-proton interaction is expected to be stronger when they are both above or both below their respective gaps, as compared to the case when one of them is below the gap and the other above it. Then one might obtain quantitative agreement with the systematics shown in figs. 9 and 10.

We conclude this section by addressing the problem of universality of the magic numbers. In fig. 12 showing Q_α systematics of heavy nuclei, the proton gap above Z = 82 is manifested as increased vertical distance between consecutive Q_α lines from Pb to Bi to Po, as compared to other elements. These larger distances attain their maximum magnitude at N = 126, decreasing on both sides of it in accordance with fig. 10. However, they persist as such down to the lightest isotopes shown in the figure with N = 106. Thus Z = 82 is magic for all presently known nuclei.

On the other hand, in lighter nuclei a larger relative change in nuclear composition results by moving smaller distances away from stability, which might result in disappearance of magicity. As a matter of fact, N = 20 is no longer magic in the very neutron-rich Na isotopes recently measured at Orsay and discussed by Dr. Detraz in this conference[11]. This is seen in the upper part of fig. 13, by comparing the S_{2n} line of Na at N = 22 with those of the heavier elements.

Even more drastically, N = 8 is no more magic in ^{11}Be, which has a $\frac{1}{2}^+$ ground state, whereas in its isotone ^{13}C the $\frac{1}{2}^-$ level from the next shell is 3.09 MeV above the $\frac{1}{2}^-$ ground state. This is illustrated in the lower part of fig. 13.

3.3. Variation of shell effects at submagic numbers

We mainly comment on the proton gaps above Z=40, 64. More complete discussion is given in ref.[12].

The lower part of fig. 14 shows Sp systematics of odd-Z nuclei near ^{90}Zr. The proton submagic gap above Z = 40 is manifested as sudden drop of isotonic Sp lines from Y to Nb. The magnitude of the drop increases from N = 48 to N = 50 and decreases from N = 50 to N = 52. Then it increases again monotonously from N = 52 to N = 56 and remains about the same in N = 58.

Likewise, the upper part of the figure shows excitation energies of the 39th proton in Y isotopes from the g.s. single-proton $\frac{1}{2}^-$ level to the single-proton $9/2^+$ level above the gap, and also excitation energies of single proton-hole $\frac{1}{2}^-$ levels from the g.s. $9/2^+$ level in Nb isotopes. The proton transition occurs in both cases across the gap into the higher $9/2^+$ subshell, and the lines of both elements indicate local maxima at N = 50, 56 in the energy changes involved, similarly to the separation energies.

Thus proton submagicity at Z = 40 is strengthened at both N = 50 and 56. This is also impressively shown in the three dimensional plots of 2^+ excitation energies shown by Dr. Pfeiffer[13] and Dr. Mattsson[14].

Like in the previous section near N = 126, Z = 82 this behaviour is not reproduced by self-consistent energy-density calculations[15].

On the other hand, the non-monotonous variation of the proton gap between N = 50 and N = 56, where the six added neutrons all preferentially enter the same $2d_{5/2}$ subshell in the ground state, seems to indicate that the neutron configuration changes considerably when the proton is excited across the gap, and that shell model calculations with mixed configurations comprising several subshells are required for explaining the systematics.

We now consider Z = 64. The lower part of fig. 15 shows Sp systematics of odd-Z nuclei near ^{146}Gd. A proton submagic gap above Z = 64 is indicated as a drop of isotonic Sp lines with N = 84 and N = 86 from Eu to Tb. However, this drop disappears in the higher-N lines.

Likewise, the upper part of the figure shows excitation energies of the 63rd proton in Eu isotopes from the single-proton g.s. $5/2^+$ level to the single-proton 11/2 level above the gap. The excitation energy attains its highest value of 716 keV for N = 82, and decreases on both sides, down to 196 keV for N = 88.

Thus both separation and excitation energies suggest a proton gap smaller than 1 MeV at N = 82, which disappears with the addition of several neutrons at N = 88. A similar conclusion is indicated by S_{2p} and Q_α systematics[16].

Fig. 16 shows S_{2p} lines for N = 50, 82, 126 nuclei and also S_{2n} line for Z = 62. These lines qualitatively indicate the magnitudes of respective gaps above Z = 40, 64, 82 and N = 82. The Z = 64 drop is the smallest, of about ½ MeV.

On the other hand, it has been claimed[17] that shell model calculations around ^{146}Gd indicate a Z = 64 proton gap about equal to the N = 82 neutron gap, being both of about 3 ½ MeV. This seems to contradict both figs. 15 and 16.

However, in ref.[17] the authors state that they actually refer to a proton-hole gap in Gd, comprising the smaller proton-particle gap indicated in the above figures and additional contribution coming from the breaking of a $|\, j^2 J = 0\rangle$ proton pair in Gd when hole-exciting it. Thus in this case there is no real contradiction.

On the other hand, level calculations[18] in ^{145}Eu with a pairing force give a proton-particle gap of 1.9 MeV. Calculations with the self consistent energy-density method[19] give 1.65 MeV.

Submagic numbers are naturally less stable than the official magic ones. We noted that the Z = 64 shell effects in the masses practically disappear at N = 88. For Z = 40 they disappear at N = 60, and for N = 56 at Z = 44. This is clearly seen in the appropriate systematics[16]. Updated versions were shown by Dr. Keyser[20].

4. Deformation

4.1. Deformation regions

As noted in sec. 2.1, semi-magic nuclei have $|j^2 J_{12} = 0\rangle$ identical-nucleon pairs in the valence shells. These are each spherically symmetric. Consequently, semi-magic nuclei do not deform.

On the other hand, the neutron-proton interaction favours many aligned neutron-proton pairs. For n neutrons and p protons in the valence shells the pairing energy increases like n + p, whereas the neutron-proton interaction is proportional to np. Consequently, when both n and p increase, one expects the neutron-proton aligning forces to win over identical-nucleon pairing forces, resulting in a breaking of the lowest seniority (pairing) approximation. When this is done in an appropriate coherent way deformation might result.

Thus one expects deformed nuclei only when both N and Z are removed from closed shells.

This agrees with experimental results on nuclear moments and isotope shifts, as discussed by Prof. Otten[21] and by Dr. Ekstrom[22], and on rotational spectra, as discussed by Drs. Pfeiffer[13], Matsson[14], Hamilton[23], Wood[24] and others at this conference.

The upper part of fig. 17 shows the three classical deformation regions known before the present active pursuit of nuclear studies far from stability started, and also those predicted then. The lower part of the figure indicates as well parts of the newer deformed regions now intensively studied. Many updated versions were shown at this conference.

Fig. 18 summarizes recent results from I_{2^+} measurements, like those shown by Prof. Otten[21] and Dr. Thibault[25]. Increased deviation from the standard straight line is interpreted as increased deformation. One observes that the semi-magic Sn isotopes (and those of the neighbouring element Cd) hardly deviate from the standard, whereas the deviation increases from Xe to Cs to Ba to Ce, parallel to the increasing number of valence neutron-(or rather neutron-hole)-proton pairs.

4.2. Change of the magic number scheme with deformation.

The development of deformation effects the masses in two ways: changing the magic and submagic numbers, and superimposing oscillations on the otherwise smooth trends between magic numbers. We discuss these respectively in this and the following section.

Magic numbers change, since in deformed nuclei the nucleons move in a deformed potential well, whose energy levels and gaps change with the deformation, like in the Nilsson scheme.

Naturally spherical submagic numbers are more affected than major magic ones. As a matter of fact, the disappearance of the Z=40 and Z=64 gaps discussed above are related to the onset of strong deformations at N=60 and N=90, respectively.

Moreover, the disappearance of magicity of N=20 in the Na isotopes also seems to be accompanied by onset of deformation , as was shown by Dr. Detraz[11]. Recent calculations[26] indicate that the disappearance of the N=8 gap in ^{11}Be might also be accompanied by deformation.

It is worth noting, that once a spherically sub-magic nucleus deforms, all spherical subshells in the major shell take part in the deformation. Thus, inspite of the submagicity of Z=64 in doubly magic ^{146}Gd, once deformation sets in around N=90, Gadolinium which is in the middle of the proton major shell between Z=50 and Z=82* deforms more than its lower Z neighbouring elements. Similarly, when deformation sets in around N=60, Zr and Sr, which are in the middle of the proton major shell between Z=28 and Z=50, deform more than their higher-Z neighbours. This is demonstrated in Fig.19, when considering the ratio E(4+)/E(2+) in even-even nuclei as criterion for deformation.

The only well established deformed magic number indicated by the masses is N=152, seen most clearly in Q_α systematics[16]. The sometimes proposed[27] submagic N=98, 104, 108 observed in selected S_{2n} systematics, likewise correspond to gaps in the Nilsson level scheme.

4.3. Oscillating trends in the masses and deformation

Between magic numbers one usually encounters oscillations in the masses. The four sheets of the mass surface oscillate independently. Consequently the distances between them oscillate as well.

Fig. 20 shows oscillating I=Const Q_α lines in the ld2s shell. These reflect the oscillations in the masses. Fig.21 shows the oscillations superposed on the otherwise smoothly decreasing with A two odd-even mass differences.

In particular, where deformation sets in suddenly, like at N=20 in the Na isotopes, at N=60 and at N=90, one observes upward kinks in the otherwise universally decreasing isotopic S_{2n} lines. These are interpreted as due to the gain in binding energy resulting from the deformation. We have seen them in the talks of Dr. Detraz[11] and Dr. Thibault[28]. The kink in the Na line is seen in fig.13.

In the shell-corrections of Myers-Swiatecki and Strutinsky the deformation energy oscillates with N and Z. This agrees with the empirical oscillations.

In the shell model there are symmetry relations between multipole matrix elements of particle-hole conjugate nuclei in a major shell, like P and Q in fig.22. As a consequence of these relations, configuration mixing within a major shell contributes oscillating terms to the energy[29].

*Add after 82: and therefore has the highest number of valence neutron-proton pairs

Deformation can be produced in the shell model only by configuration mixing which violates the seniority (pairing) scheme. Thus, in a deformed region one expects the masses to oscillate from shell model considerations as well.

On the other hand, there is configuration mixing in semi-magic nuclei as well, like the Sn isotopes. However, according to the analysis in sec. 4.1 such nuclei do not deform.

In S_{2n} systematics[16] the line of the spherical Sn isotopes oscillates slightly, to about the same extent as the line of the light Cs isotopes, which are somewhat deformed, as indicated in fig. 18.

Thus, while deformation makes the masses oscillate, mild oscillations in the masses do not necessarily imply deformation.

I am indebted to Dr. Pfeiffer for ref.13 and to Dr. Åberg for ref. 26.

References

1. J.P.Schiffer, Annals of Physics 66 (1971) 798
2. N.Zeldes and S.Liran, Physics Letters 62B (1976) 12.
3. M.Danos and V.Gillet, Z.Physik 249 (1972) 294 and references there.
4. A.Arima and V.Gillet, Annals of Physics 66 (1971) 117.
5. N.Zeldes and A.Taraboulos, Notas de Fisica 1, No.9 (1978) 271.
6. M.Chakraborty, V.K.B.Kota and J.C.Parikh, Phys. Rev.Letters 45 (1980) 1073 and references there.
7. M.Cauvin, V.Gillet and F.Soulmagnon, Nuclear Physics A361 (1981) 192.
8. C.Y.Tseng, T.S.Cheng and F.C.Yang, Nuclear Physics A334 (1980) 470.
9. K.H.Schmidt and D.Vermeulen, Atomic Masses and Fundamental Constants 6, J.Nolen and W.Benenson,eds. (Plenum Press, 1980) p.119 and references there.
10. R.A.Sorensen, these Proceedings, and references there.
11. C.Détraz, these Proceedings.
12. N.Zeldes, International Workshop on Gross Properties of Nuclei and Nuclear Excitations VII B: Nuclei far off β-stability, H.v.Groote, ed (TH Darmstadt, 1979) 56.
13. B.Pfeiffer, E.Monnand, J.A.Pinston, F.Schussler, G.Jung, J.Münzel and H.Wollnik, these Proceedings.
14. S.Matsson, R.E.Azuma, H.A.Gustafsson,P.G.Hansen, B.Jonson, V.Lindfors, G.Nyman and D.Schardt, these Proceedings.
15. M.Beiner, R.J.Lombard and D.Mas, Atomic Data and Nuclear Data Tables 17 (1976) 450.
16. K.Bos and A.H.Wapstra, Atomic Data and Nuclear Data Tables 19 (1977) 277.
17. P.Kleinheinz, R.Broda, P.J.Daly, S.Lunardi, M.Ogawa and J.Blomqvist, Z.Physik A290(1979)279.
18. R.R.Chasman, Phys.Rev. C21 (1980) 456.
19. F.Tondeur, Nuclear Physics A338 (1980) 77.
20. U.Keyser, F.Münnich, B.Pahlmann and B.Pfeiffer, these Proceedings.
21. E.W.Otten, these Proceedings.
22. C.Ekström, these Proceedings.
23. J.Roth, L.Cleemann, J.Eberth, T.Heck, W.Neumann, M.Nolte, R.B.Piercey, A.V.Ramayya and J.H. Hamilton, these Proceedings.
24. J.L.Wood, these Proceedings.
25. C.Thibault, F.Touchard, S.Büttgenbach,R.Klapisch, M.de Saint-Simon, J.M.Serre, P.Guimbal,H.T.Duong, P.Jacquinot, P.Juncar, S.Liberman, P.Pillet,

J.Pinard, J.L.Vialle, A. Pesnelle, and G.Huber, these Proceedings and Phys. Rev. C23 (1981) 2720
26. I. Ragnarsson, T.Bengtsson and S.Åberg, XIX International Winter Meeting on Nuclear Physics, Bormio, 1981. (Lund-MPh-81/03)
27. R.C.Barber, J.O.Meredith, F.C.G.Southon, P.Williams,J.W.Barnard, K.Sharma and H.E.Duckworth, Phys.Rev.Letters 31(1973)728.
28. M.Epherre, G.Audi, C.Thibault,R.Klapisch, G.Huber, F.Touchard and H.Wollnik, these Proceedings and Phys.Rev. C19 (1979)1504.
29. S.Liran and N.Zeldes, ref. 15, p. 431.
30. V.Cappeller, Nuclear Masses and their Determination, H.Hintenberger, ed. (Pergamon,1957)27.
31. N. Zeldes, ref. 9, p. 129.
32. N.Zeldes and S.Liran, Atomic Masses and Fundamental Constants 5, J.H.Sanders and A.H.Wapstra, eds. (Plenum Press, 1976) 264.
33. N.Zeldes, Atomic Masses and Fundamental Constants 4, J.H.Sanders and A.H.Wapstra, eds. (Plenum Press, 1972) 245.
34. C.Thibault, M.Epherre, G.Audi, R.Klapisch, G.Huber, F.Touchard, D. Guillemaud and P.Naulin, ref. 9, p. 291.
35. I.Talmi and I.Unna, Phys.Rev.Letters 4(1960) 469.
36. L.Spanier, S.Z.Gui, H.Hick and E.Nolte, Z. Physik A299(1981) 113
37. E.Marshalek, L.W.Person and R.K.Sheline, Rev. Mod. Phys. 35 (1963) 108
38. A.Bohr and B.R.Mottelson, Nuclear Structure, Vol. II (Benjamin,1975) p. 27.
39. H.A.Schuessler, Physics Today, February 1981, p. 48.
40. J.B. Wilhelmy, S.G. Thompson, R.C. Jared and E. Cheifetz, Phys.Rev.Letters 25(1970)1122.
41. H.Wollnik, F.K. Wohn, K.D.Wünsch and G.Jung, Nuclear Physics A291 (1977) 355.
42. E.Comay, S.Liran, J. Wagman and N.Zeldes, International Conference on the Properties of Nuclei far from the Region of Beta-Stability, Leysin, 1970 (CERN 70-30) 165.
43. A.Bohr and B.R.Mottelson, ref. 38, Vol. I (Benjamin, 1969) p. 170.
44. F.Ajzenberg-Selove, Nuclear Physics A 320 (1979)1.
45. C.M. Lederer and V.S.Shirley, Eds., Table of Isotopes, 7th Edition (Wiley, 1978) and more recent literature.
46. A.H. Wapstra and K. Bos, ref. 16, pp. 177, 215 and more recent literature.

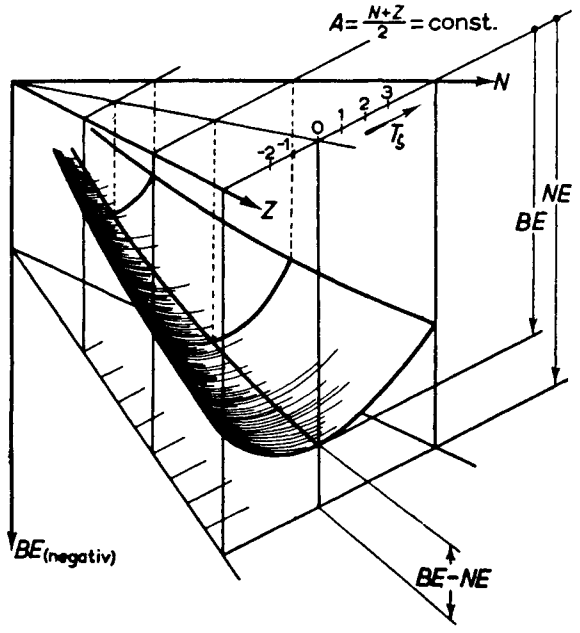

Fig. 1 Gross appearance of the nuclear mass surface[30]

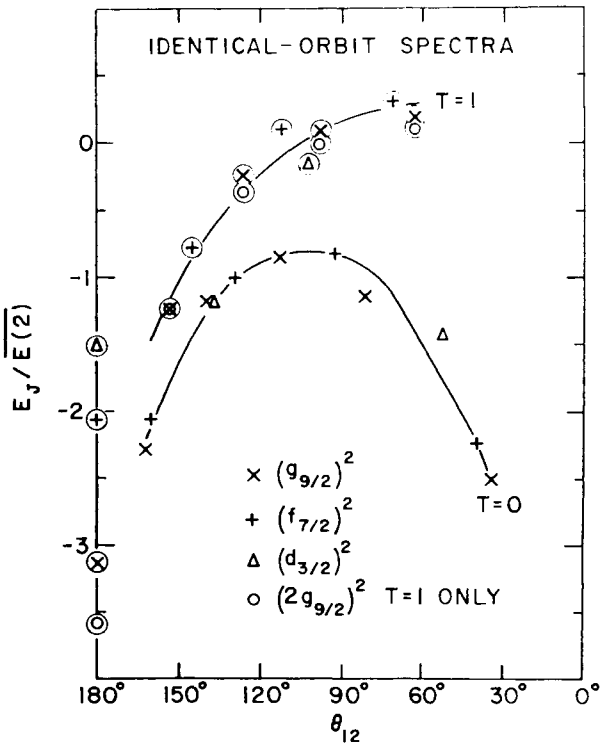

Fig. 2 Effective interaction matrix elements of equivalent nucleons[1]

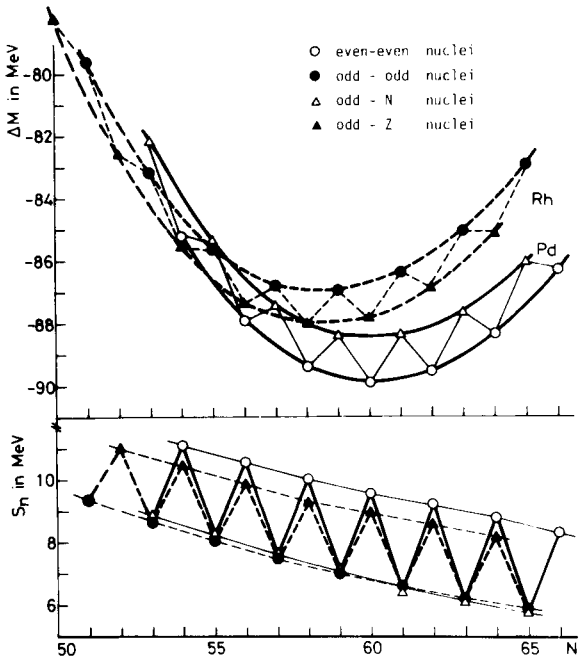

Fig. 3 Mass parabolas above and neutron separation energies below for Rh and Pd nuclei [51]

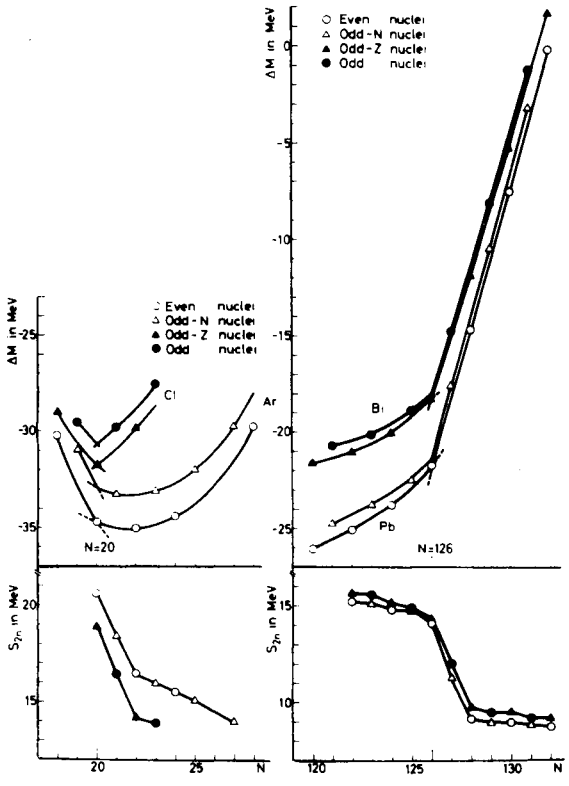

Fig. 5 Mass parabolas above and two-neutron separation energies below for Cl, Ar, Pb and Bi nuclei [32]

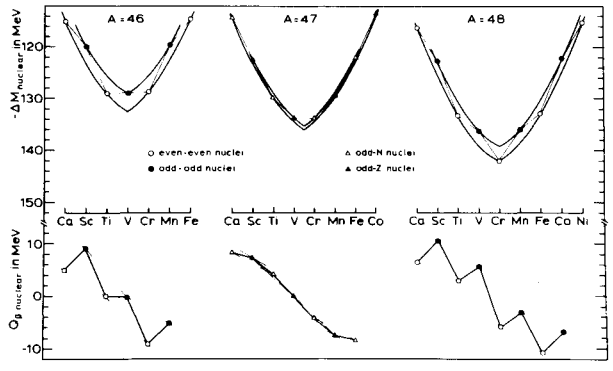

Fig. 4 Mass excesses above and Q_β-values below for $1f_{7/2}$ isobars, with Coulomb energy and neutron-proton mass differences subtracted [31]

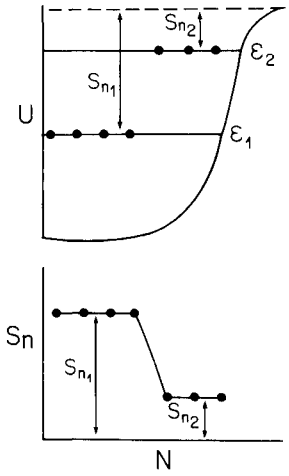

Fig. 6 (a) Single neutron levels in a schematic nuclear potential and their relation to neutron separation energies, neglecting nucleon interactions and rearrangement

(b) Neutron separation energies in a chain of successive isotopes, starting from the neutron configuration shown in (a).

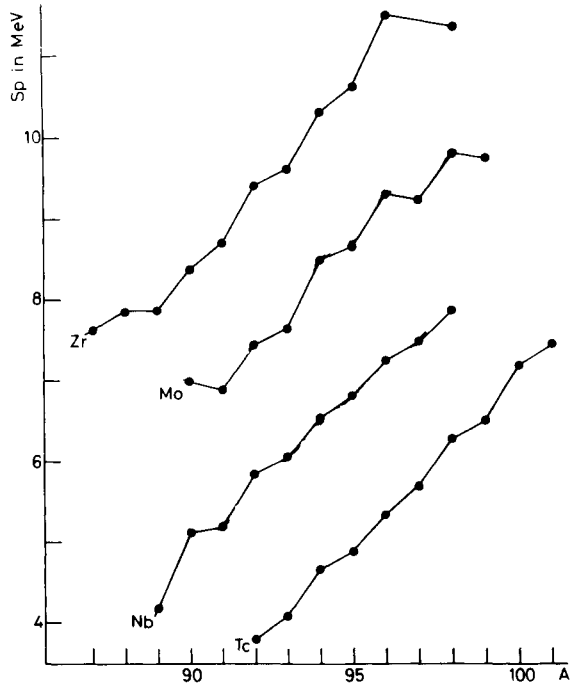

Fig. 7 Sp as function of N for Zr, Nb, Mo and Tc nuclei[33]

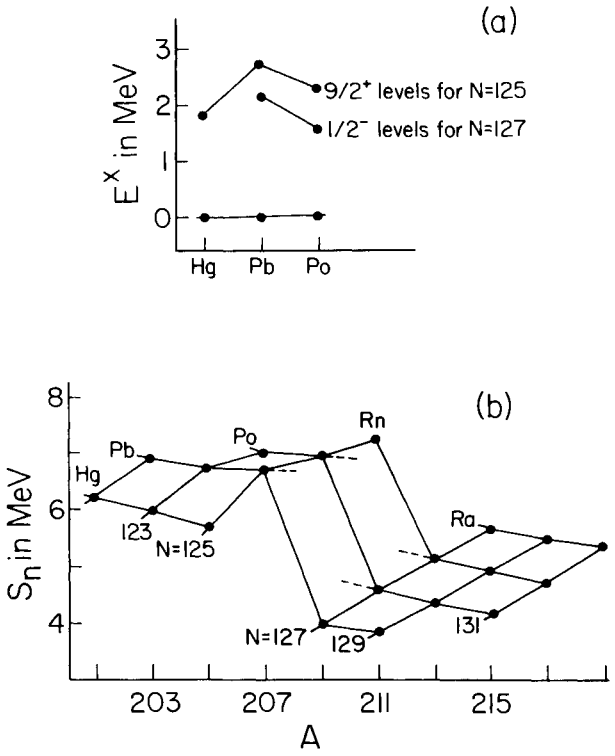

Fig. 9 (a) Excitation energies of single-neutron $9/2^+$ levels in N=125 nuclei and of single neutron-hole $\frac{1}{2}^-$ levels in N =127 nuclei[45]

(b) Sn systematics of odd-N nuclei near ^{208}Pb.[46]

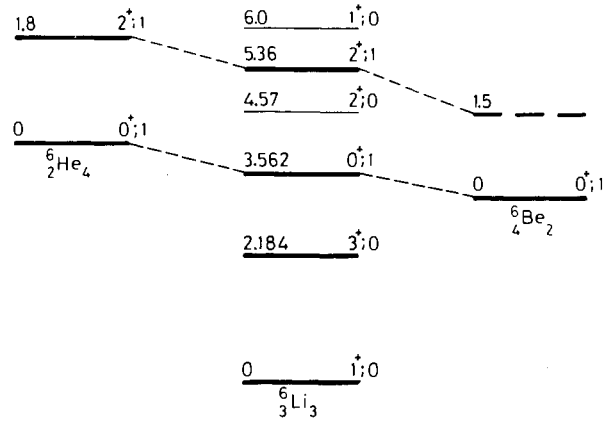

Fig. 8 Levels of the $1p_{3/2}^2$ nuclear configuration in A=6 isobars[44]

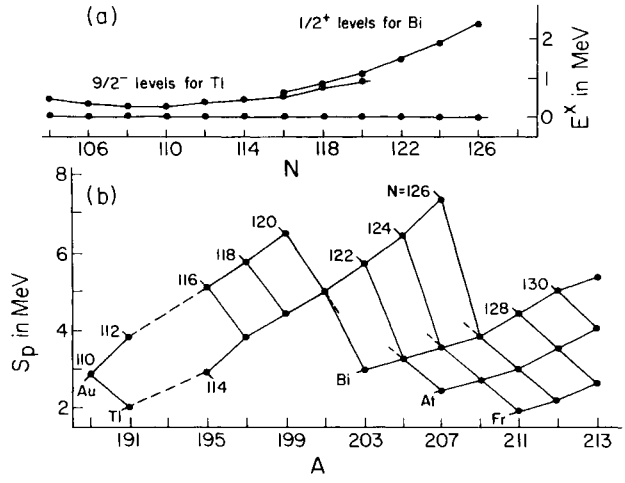

Fig. 10 (a) Excitation energies of single-proton $9/2^-$ levels in Tl isotopes and of single proton-hole $\frac{1}{2}^+$ levels in Bi isotopes.[45]

(b) Sp systematics of odd-Z nuclei near ^{208}Pb.[46]

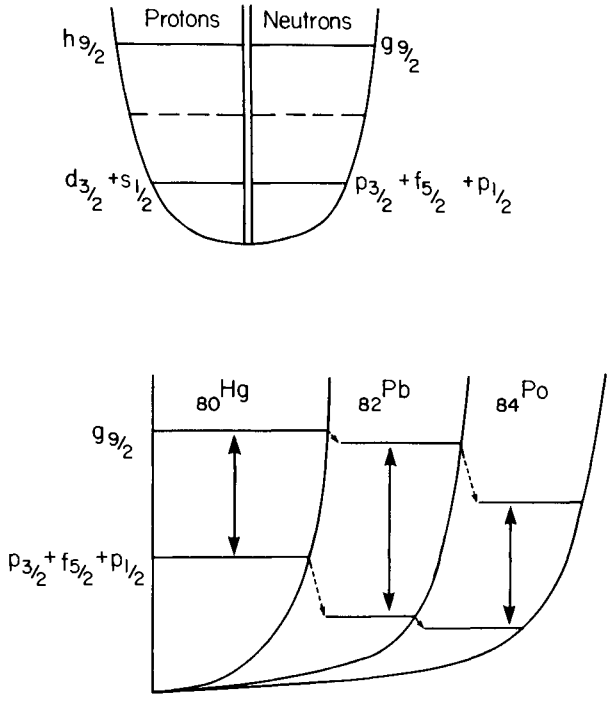

Fig. 11 (a) Schematic description of single-nucleon levels just below and above the magic gaps near ^{208}Pb.

(b) Interpretation of the mutual support of magicities near ^{208}Pb in an independent particle picture

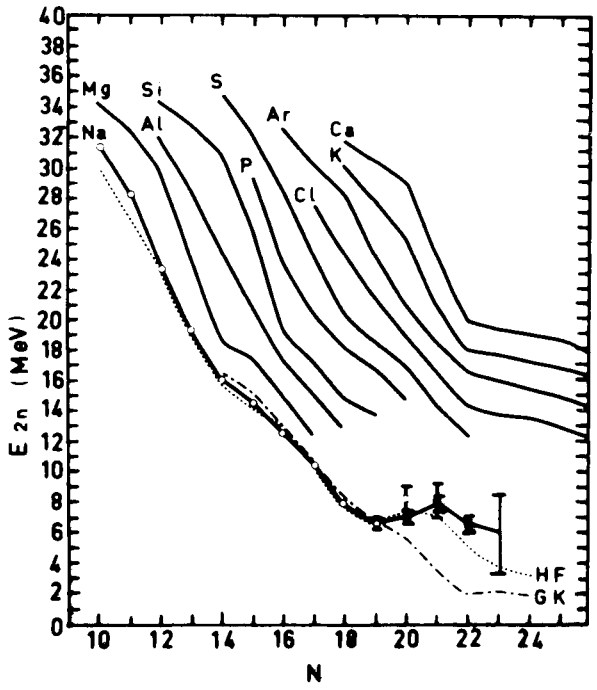

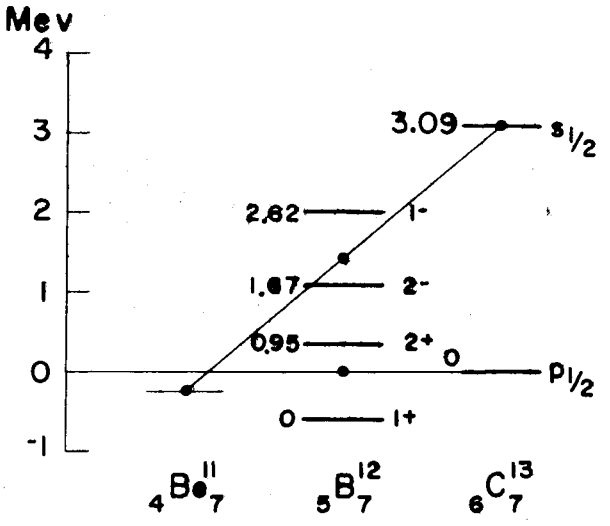

Fig. 13 above: Two neutron separation energies around N = 20 in Na and in heavier elements[34]

below: Competition between the $1p_{1/2}$ and $2s_{1/2}$ shells[35]

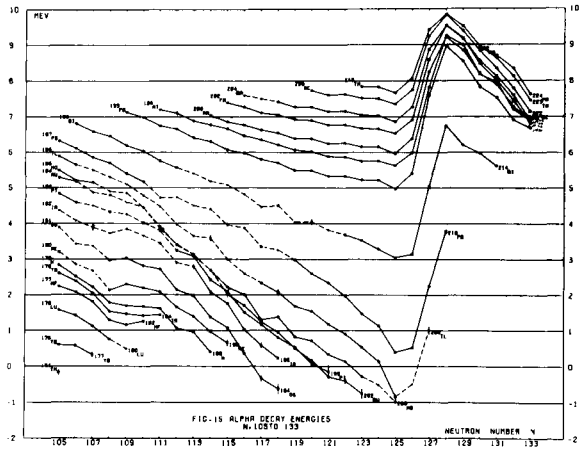

Fig. 12 Q_α systematics of heavy nuclei[16]

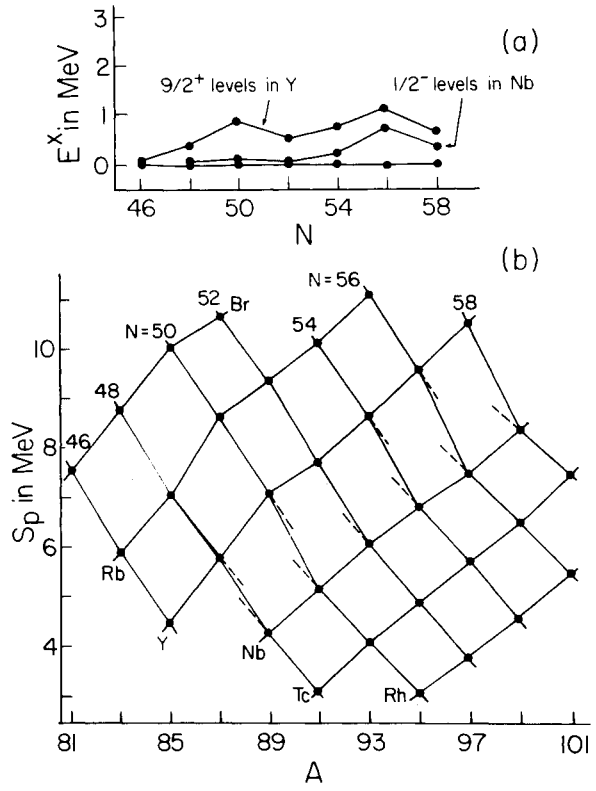

Fig. 14 (a) Excitation energies of single-proton $9/2^+$ levels in Y isotopes and of single proton-hole $\frac{1}{2}^-$ levels in Nb isotopes.[45]

(b) S_p systematics of odd-Z nuclei near $^{90}_{40}Zr$.[46]

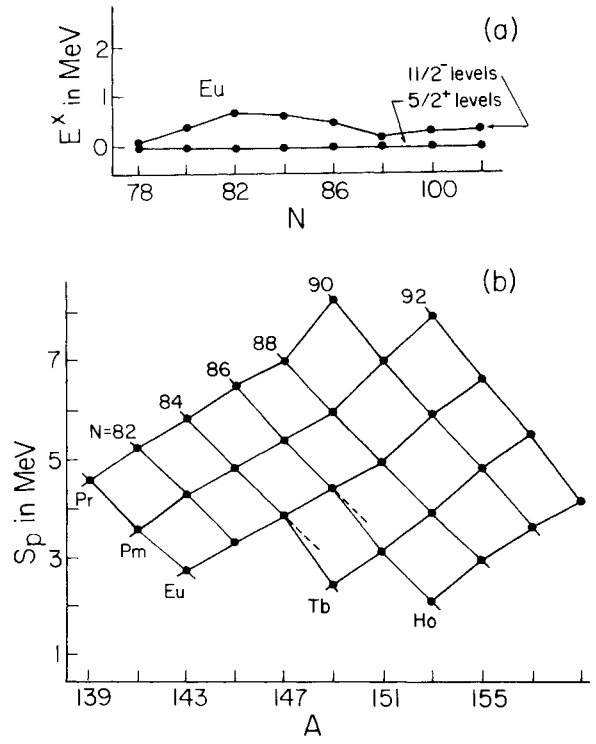

Fig. 15 (a) Excitation energies of single-proton $11/2^-$ levels in Eu isotopes[45]

(b) S_p systematics of odd-Z nuclei near ^{146}Gd.[46]

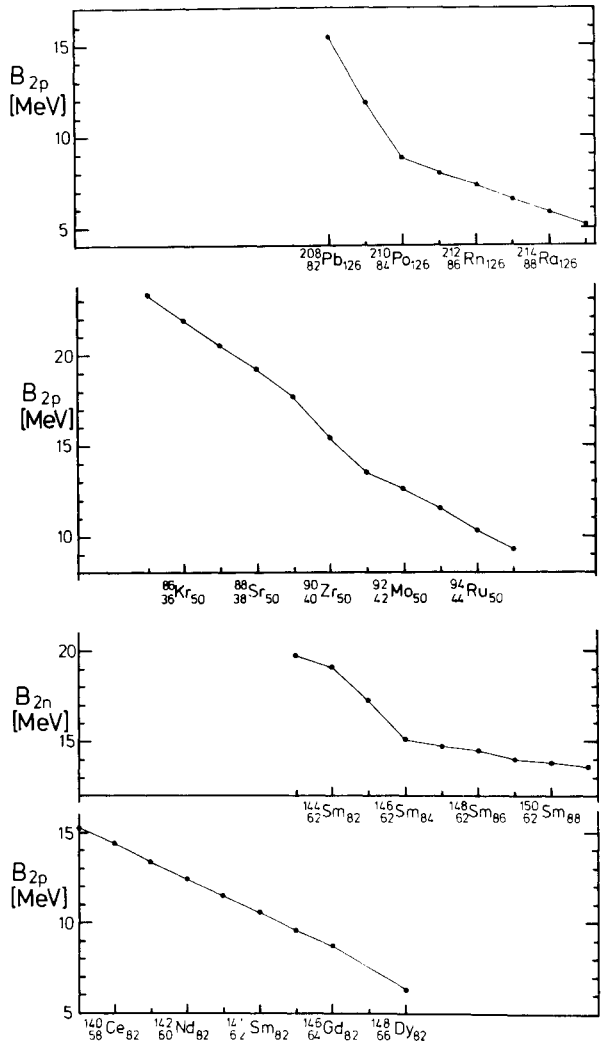

Fig. 16 From top to bottom: S_{2p} lines for N = 126 and for N = 50, S_{2n} line for Z = 62, S_{2p} line for N = 82, reference 36.

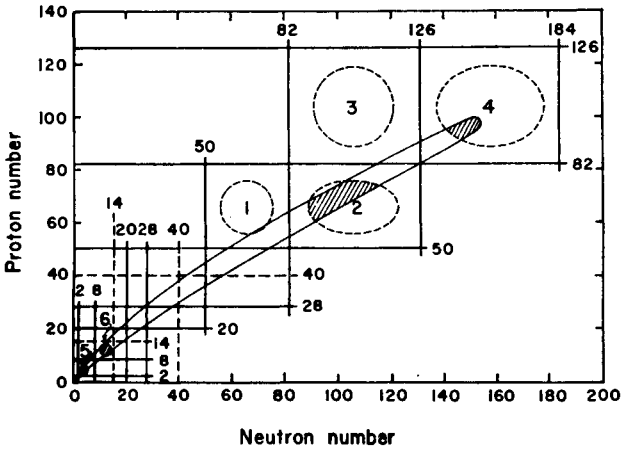

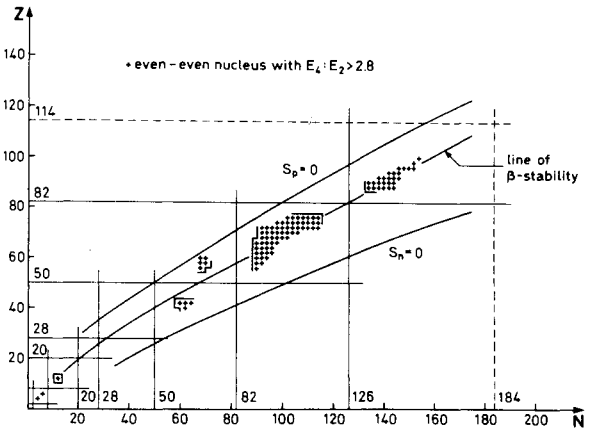

Fig. 17 above: Deformation regions known and expected in 1963[37]

below: Deformation regions known in 1975[38]

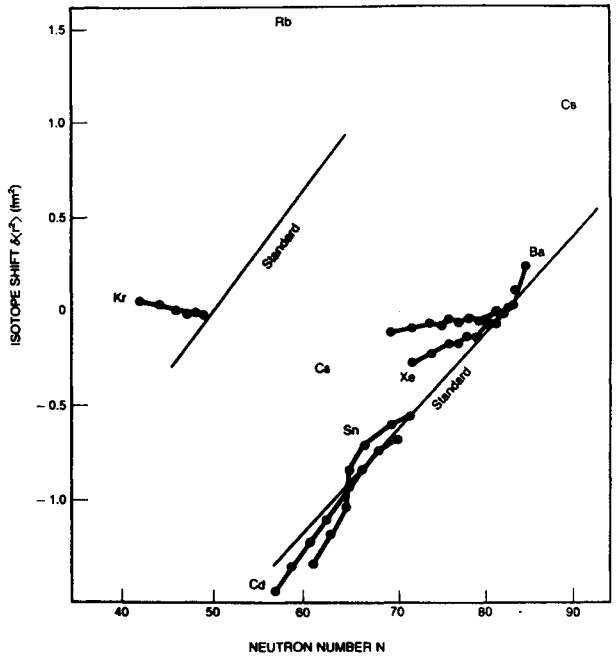

Fig. 18 Relative charge radii in chains of isotopes extending far from stability[39]

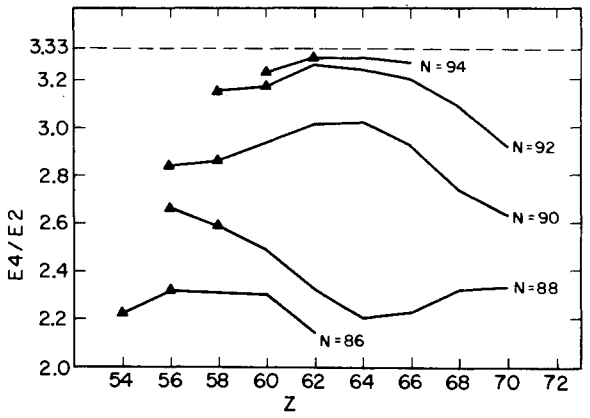

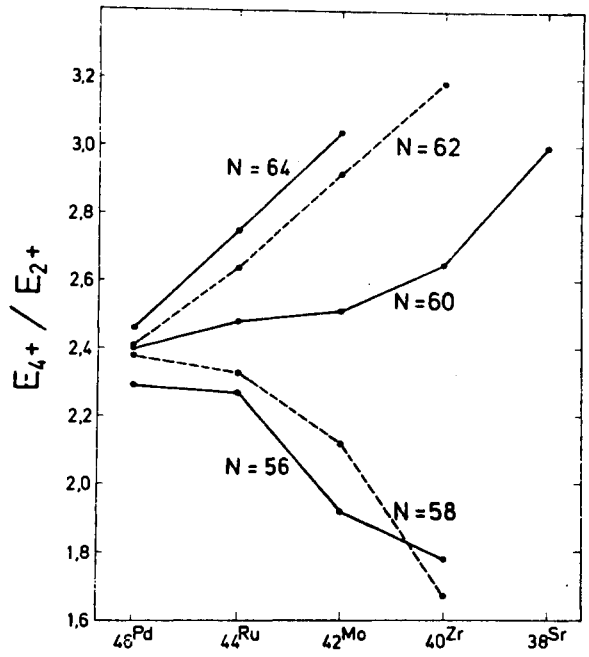

Fig. 19 Ratios of excitation energies $E(4_1^+)/E(2_1^+)$ in even-even nuclei.

above: for N = 86-94 isotones[40]

below: for N = 56-64 isotones[41]

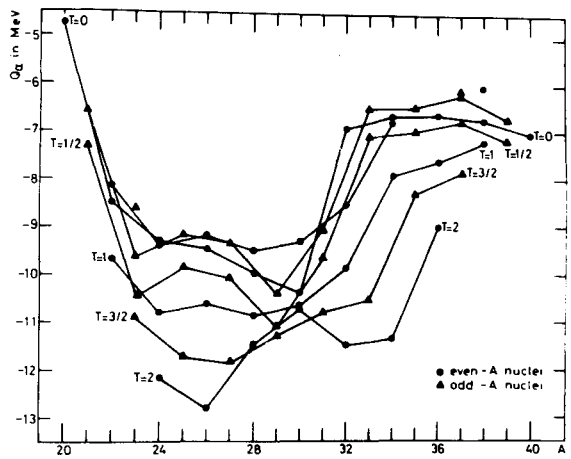

Fig. 20 Q_α systematics in the 1d2s shell.[42]

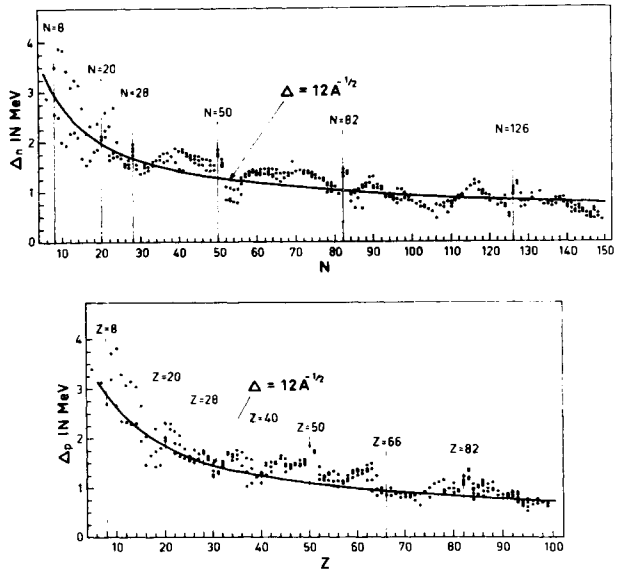

Fig. 21 Odd-even mass differences[43)]

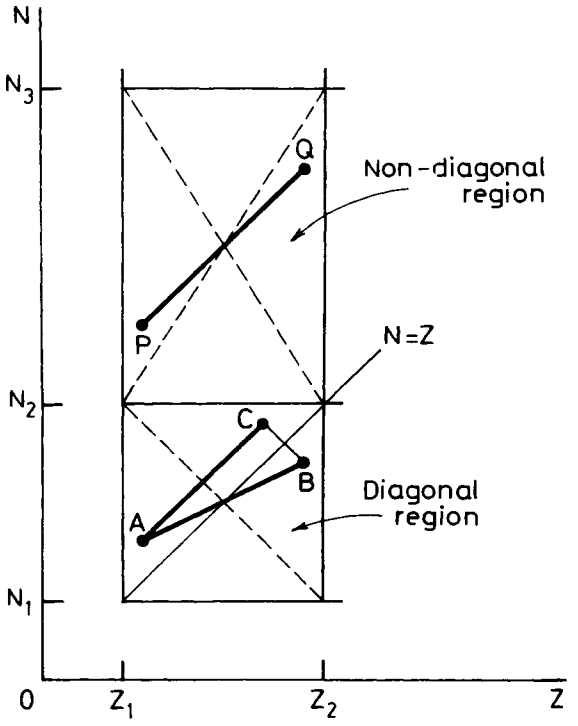

Fig. 22 Particle-hole conjugate nuclei in diagonal shell regions, A and B, and in non-diagonal regions, P and Q.

DISCUSSION

J.R. Nix: 1) You have discussed in a qualitative way the empirical appearance of the nuclear mass surface. But does your approach have any predictive power for telling us the mass or deformation of a nucleus for which these quantities have not yet been measured? 2) How many adjustable parameters are there in your approach?

N. Zeldes: 1) It has a predictive power for telling masses, as was shown by Dr. Thibault yesterday morning. It cannot predict deformations. 2) About 180 adjustable parameters, divided among 10 shell regions.

K. Bleuler: The energy-gap at the magic neutron number does not depend only on the energies of the single-particle levels; it is strongly influenced (i.e. diminished or reduced by about 2-3 MeV) by the effects of pairing (BCS) theory. This effect depends strongly on the level-density which in turn depends via the proton-neutron interaction on the proton levels. For a magic proton-number this density is strongly reduced and hence the (negative) effect on the gap at the magic neutron-number is also diminished.

N. Zeldes: It seems to me that the effect that you mention will be much too small, and in order to reproduce the data one has to consider the neutron-proton interaction in a more direct way by first-order perturbation theory, similarly to the consideration of identical-nucleon pairing by BCS theory.

T. Huus: The odd-even oscillations you have discussed are seen very clearly in this viewgraph of odd-A beta decay energies as function of A, where the lines connect nuclei of constant N-Z, which shows that they are caused by shell-effects in the pairing energy. The breaking of a neutron pair is not compensated by the formation of a proton pair, when either the neutrons or the protons are near to a closed shell, where fewer levels are available for coupling by the pairing interaction. Similar effects occur for unpaired nucleons due to blocking, and solving the pairing equations for a simplified level distribution yields oscillations which qualitatively agree with the empirical oscillations.

N. Zeldes: The viewgraph indeed nicely illustrates oscillations of the distance between the two odd-A surfaces as due to mixing of subshells within major shells.

S. Åberg: I would like to make a comment concerning your discussion about the disappearance of the N=8 gap. I think that nuclear deformation provides a natural way to understand the low-lying positive-parity states in the N=7 isotopes you showed. Thus, still with a big spherical N=8 gap, calculations in Lund show that the positive-parity state in $^{11}_{4}Be_7$ is lowered by about 12 MeV by getting deformed ($\varepsilon \approx 0.7$, $\gamma \approx 35°$), while the negative parity state comes out at a much smaller deformation ($\varepsilon \approx 0.3$, $\gamma \approx 0°$) and is then only lowered by about 2 MeV relative to the sphere. This deformation change is caused by the excitation of only one neutron, from the deformation preventing $p_{1/2}$ orbital to the very deformation driving $d_{5/2}$ orbital [220½]. In a similar way, now by also adding one or two protons in the deformation preventing $p_{3/2}$ orbital [101$^{3}/_{2}$], one can also understand why in $^{12}_{5}Be_7$ and $^{13}_{6}C_7$, the positive-parity state is somewhat pushed up and comes above the negative-parity state.